33. Field-Effect Transistor 3

- β-(Al_xGa_{1-x})₂O₃/Ga₂O₃ modulation-doped field effect transistors

Yuewei Zhang¹, Sriram Krishnamoorthy², Siddharth Rajan³

- ¹ Materials Department, University of California, Santa Barbara, California 93106, USA. Email: yueweizhang@ucsb.edu
- ² Electrical and Computer Engineering, The University of Utah, Salt Lake City, UT 84112 USA. Email: sriram.krishnamoorthy@utah.edu
- ³ Electrical and Computer Engineering, The Ohio State University, Columbus, OH 43210 USA. Email: raian.21@osu.edu

Index: MODFETs, 2DEG, mobility, saturation velocity, field effect transistors, modulation doping, electrical breakdown, electrical transport, alloy, heterostructure, quantum oscillation, quantum transport, quantum well, DH-MODFETs, field effect mobility, RF characteristics, cut-off frequency, power electronics, RF electronics, transconductance, MBE, delta-doping, conduction band offset, regrown contacts, scattering.

Abstract: The availability of monoclinic aluminum gallium oxide (β-(Al_xGa₁- $_x)_2O_3)$ alloys and their staggered band alignment with β -Ga $_2O_3$ makes it possible to realize two-dimensional electron gas (2DEG) through modulation-doping. This brings unique advantages in improving the electrical transport properties in β-Ga₂O₃, and at the same time, it provides a great platform for the evaluation of a range of the fundamental materials and electrical properties of β-Ga₂O₃. In this chapter, we describe the early efforts in the design and epitaxy of the heterostructures, and discuss the confirmation of a 2DEG through temperature-dependent Hall measurements as well as the first observation of the quantum oscillations in the material system. We will further discuss the realization of modulation-doped field effect transistors (MODFETs), which have contributed to the evaluation of the saturation velocity and demonstration of high breakdown field in the material system. We will also discuss the methods to improve the 2DEG density, and present the first double heterostructure MODFET (DH-MODFET). The early efforts on β-(Al_xGa₁x)2O3/ Ga2O3 heterostructures confirmed that the modulation-doped structure could be a promising architecture for electronic device applications.

Introduction

Beta-phase gallium oxide (β-Ga₂O₃) has been recognized recently as a promising candidate for electronic device applications because of its wide band gap energy (4.6 eV) and the expected high breakdown field near 8 MV/cm². This, together with good doping properties, ohmic contacts, and a relatively high estimated saturation velocity of $\sim 2 \times 10^7$ cm/s³, leads to a high figure of merit for both power electronics and high-frequency electronics applications. Moreover, the availability of high quality single-crystal material using melt-based techniques⁴⁻⁶ is beneficial for mass production of low-defect wafers, especially when compared to other wide bandgap semiconductors, such as SiC and GaN. Recent efforts have led to the demonstration of various device structures with promising device performance.⁷⁻¹⁷ Experimental observations of high breakdown fields above 5 MV/cm have been reported for vertical Schottky diodes^{18,19}, and near 4 MV/cm for lateral MOSFET transistors²⁰, which have already surpassed the material limit for GaN and SiC. Current modulation and the capability toward high frequency operations were demonstrated as well. However, most of the existing research relied on bulk-doped β-Ga₂O₃ channels, leading to low transconductance (g_m). Besides, the on-resistance and the ability to operate under velocity saturation regime have also been limited by the low channel mobility below 150 cm²/Vs at room temperature mainly due to polar optical phonon scattering. These issues greatly limit the applications of β-Ga₂O₃ in both power and high-frequency devices.

Improvements in the electron mobility is feasible in a modulation-doped two-dimensional electron gas (2DEG) channel by reducing the effect of ionized impurity scattering. Theoretical calculations predicted an enhanced screening effect for high 2DEG densities above 5×10^{12} cm⁻², and this could lead to an improved channel mobility above 500 cm²/Vs at room temperature.²¹ The higher channel mobility could bring significant research opportunities for β -Ga₂O₃ in a range of device applications. Additionally, the 2DEG channel provides the feasibility for charge scaling and aggressive device scaling in both lateral and vertical directions, making it especially favorable for high frequency electronics and power switching applications.

In this chapter, we will review the early development of AlGaO/GaO modulation-doped field effect transistors (MODFETs) and discuss the design and experimental confirmation of the 2DEG channel at the heterointerface. The modulation doped structures were further used to determine several electronic properties of β -Ga₂O₃, including low-field transport properties in a wide temperature range, quantum transport, electron saturation velocity in β -Ga₂O₃ and breakdown strength.

Monoclinic phase (AlGa)₂O₃ forms a staggered band alignment to β -Ga₂O₃, with a positive conduction band offset and small valence band offset. ²² When a thin sheet of dopants is placed in the (AlGa)₂O₃ layer, the free carriers could be transferred to the AlGaO/GaO interface²³, leading to the formation of a 2DEG. The equilibrium 2DEG density (n_s) in the system is determined by electrostatics and can be estimated by

$$n_s = \frac{eN_d^+ d_{\delta} - \varepsilon(\phi_b - \Delta E_c/e)}{eD}, (1)$$

where N_d^+ , ϕ_b , and ΔE_c represent the activated donor concentration in the delta-doped layer, the Schottky barrier height and the conduction band offset, respectively. e and ε are the unit charge and dielectric constant. The physical definitions for the thicknesses d_δ and D are schematically shown in Fig. 1(a). For 2DEG densities above 10^{12} cm⁻², the contribution from the second term of equation (1) is negligible and the 2DEG density is mainly determined by the first term. Therefore, more charge could be transferred to the 2DEG channel when the spacer thickness is reduced. Increasing the intentional doping concentration could lead to a similar increase of the 2DEG density until the onset of a parasitic channel formed in the (AlGa)₂O₃ barrier layer. The low conductivity in the parasitic channel could compromise the overall conductivity of the modulation-doped structure and impact the device performance. Therefore, significant effort has been devoted to the optimization of the modulation-doped structures to avoid the formation of the parasitic channel, and this also sets an upper limit on the pure 2DEG density for a given conduction band offset.

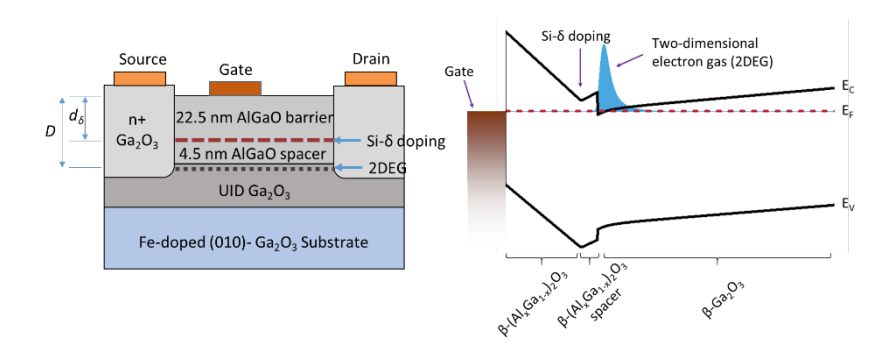


Figure 1 (a) Schematic structure for the modulation-doped field effect transistor. (b) Schematic energy band diagram of the MODFET. A 2DEG is formed at the AlGaO/GaO interface through modulation doping.

Alloying of Al with β -Ga₂O₃ provides flexibility for heterostructure device designs. β -(Al_xGa_{1-x})₂O₃ has been demonstrated to be stable with Al composition up to 80%, even though Al₂O₃ is stable in the corundum polytype. Epitaxial growth of β -(Al_xGa_{1-x})₂O₃ has been attempted by several growth techniques, including molecular beam epitaxy (MBE)²⁵⁻²⁸, pulsed laser deposition (PLD)²⁹⁻³², mist chemical vapor deposition (CVD)³³ and metal-organic chemical vapour deposition (MOCVD)³⁴. Because of the atomic layer precision, controlled n-type doping provided by MBE growth and maturity in the growth technique, it was the first technique used for the realization of the MODFET structures. ^{13,16,17}

The MBE growth condition of β-(Al_xGa_{1-x})₂O₃ was first explored by Takayoshi Oshima et al on (100)-oriented β-Ga₂O₃ substrates²⁶. At a substrate temperature of 800 °C, an Al composition up to 61% was achieved. However, the films showed high surface roughness, and at the same time, the growth on (100)-oriented substrates suffered from significantly lower growth rate compared to the growth on (010)-oriented substrates since it is a cleavage plane and has higher desorption rate at the growth temperatures. β-(Al_xGa_{1-x})₂O₃ growth on (010)-oriented substrates was investigated by Stephen Kaun et al²⁵, who demonstrated smooth surface morphology and sharp heterointerfaces between β-(Al_xGa_{1-x})₂O₃ and β-Ga₂O₃. However, the maximum Al composition achieved in the monoclinic phase was found to be less than 25%, which was further confirmed by other researchers. This limits the conduction band offset at the AlGaO/GaO interface below 0.4 eV.²² As a result, the maximum 2DEG density that can be confined at the heterointerface before the onset of the parasitic channel in the AlGaO barrier layer is estimated to be $\sim 2 \times 10^{12}$ cm⁻² for the structure shown in Fig. 1(a), which has a 4.5 nm spacer layer and 22.5 nm AlGaO barrier above the delta-doped layer.

Preliminary demonstrations on β -(Al_xGa_{1-x})₂O₃/Ga₂O₃ modulation-doped field effect transistors have been reported by several groups using either Si-delta doping or Ge doping in the β -(Al_xGa_{1-x})₂O₃ layer or Garrier confinement was demonstrated based on capacitance-voltage measurements. Or However, high sheet charge densities above 5×10^{12} cm⁻² were measured for the channels, suggesting the existence of a parasitic channel in the AlGaO barrier layer. This was further confirmed by the absence of an improvement of the channel mobility, which could have been reduced by parallel conduction through the low mobility channel in the (Al_xGa_{1-x})₂O₃ layer.

Development of the β -(Al_xGa_{1-x})₂O₃/Ga₂O₃ modulation-doped structures by Y. Zhang et al^{15,17,36} focused on the optimization of the intentional doping concentration in the AlGaO barrier layer to avoid the formation of a parasitic channel. The Si delta doping concentration was controlled by varying both the cell temperature and the shutter pulsing time during growth.¹⁷ The impurity distribution within one monolayer of (Al_xGa_{1-x})₂O₃ was expected. Successes in the removal of the parasitic channel led to the demonstration of single 2DEG channels with densities below 2×10^{12} cm⁻². This allowed for the characterization of the intrinsic 2DEG transport properties in β -Ga₂O₃.

Electrical transport in AlGaO/GaO MODFETs

In this section, we discuss the characterization of a 2DEG at the AlGaO/GaO interface through the measurement of the electrical transport characteristics of the structure. Similar to the other 2DEG systems in AlGaAs/GaAs MODFET or AlGaN/GaN HEMT structures, the 2DEG carrier density is expected to have weak

temperature dependence because of the electrostatics. At the same time, the reduced impact from polar optical phonon scattering is expected to enable superior transport characteristics at cryogenic temperatures. Therefore, unique quantum transport properties of the 2DEG are anticipated in the AlGaO/GaO modulation doped structure. In this section, we discuss direct evidences of quantum confinement of a 2DEG at the β -(Al_xGa1-x)_2O_3/Ga2O_3 interface based on temperature-dependent Hall measurements and Shubnikov-de Haas (SdH) oscillations.

The modulation-doped $\beta\text{-}(Al_xGa_{1-x})_2O_3/Ga_2O_3$ structure is shown in Fig. 1. To achieve ohmic contact, a degenerately-doped $\beta\text{-}Ga_2O_3$ layer was grown to enable sidewall contact to the electron channel. ^17,37 A metal stack of Ti/Au was then evaporated on the regrown Ga_2O_3 regions and annealed at 470 °C for 1 min to form ohmic contact. TLM measurement for the source/drain contacts indicated ohmic performance with contact resistivity of $\sim 9~\Omega$ mm to $\sim 1~\Omega$ mm depending on the total charge density in the channel. ^15,17,37 The degenerate doping in the $\beta\text{-}Ga_2O_3$ contact layer prevented carrier freeze-out and ensured ohmic contact at cryogenic temperatures.

The temperature-dependence of Hall charge density and Hall mobility was measured using a Van der Pauw structure, as shown in Fig. 2. Weak temperature dependence in the measured Hall charge density was observed for the modulation-doped structures. This is in contrast with the carrier freeze-out in bulk-doped $\beta\text{-}Ga_2O_3$ at low temperatures $^{38\text{-}40}$, and serves as a direct proof of a degenerate 2DEG at the $\beta\text{-}(Al_xGa_{1-x})_2O_3/Ga_2O_3$ interface. One challenge that needs to be addressed is the possible appearance of a parasitic channel in the $(Al_xGa_{1-x})_2O_3$ barrier layer because of the difficulty in the intentional doping control. It was experimentally observed that the 2DEG density that can be confined in the adopted AlGaO/GaO modulation doped structure with Al composition of $\sim 18\%$ (Fig. 2) is approximately $\sim 2\times10^{12}$ cm 2 because of the small conduction band offset, which was predicted to be less than 0.4 eV based on first principle calculations. Further increase in the 2DEG charge density requires higher conduction band offset or using a relatively thinner spacer layer.

The room temperature mobility of $180\,\mathrm{cm^2/Vs}$ was measured in a modulation-doped structure. This is similar to the highest reported values in lightly-doped bulk β -Ga₂O₃ films.³⁹ The channel mobility increased significantly upon lowering the measurement temperature, and a low temperature mobility value of 2790 cm²/Vs was obtained in the β -Ga₂O₃ material system. To understand the scattering mechanisms, the temperature dependence of electron mobility was analyzed by considering various scattering mechanisms, including polar optical phonon scattering (μ_{POP}), remote impurity scattering (μ_{RS}), background impurity scattering ($\mu_{background}$), acoustic deformation potential scattering (μ_{ADP}), interface roughness scattering (μ_{IFR}) and alloy scattering (μ_{Alloy}). The total effective mobility was obtained based on Matthiessen's rule: $1/\mu_{eff} = 1/\mu_{RS} + 1/\mu_{background} + 1/\mu_{POP} + 1/\mu_{ADP} + 1/\mu_{IFR} + 1/\mu_{Alloy}$.

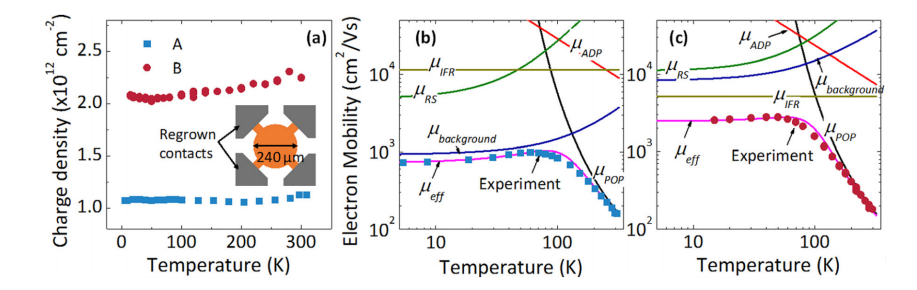


Figure 2 (a) Temperature-dependence of charge density measured using a Van der Pauw configuration as shown in the inset. (b-c) Experimental and calculated electron mobilities for sample A (b) and sample B (c) by considering various scattering mechanisms, including: polar optical phonon scattering (μ_{POP}), remote impurity scattering (μ_{RS}), background impurity scattering ($\mu_{background}$), interface roughness scattering (μ_{IFR}), and acoustic deformation potential scattering (μ_{ADP}). Reproduced from Y. Zhang, A. Neal, Z. Xia, C. Joishi, J. Johnson, Y. Zheng, S. Bajaj, M. Brenner, D. Dorsey, K. Chabak, G. Jessen, J. Hwang, S. Mou, J. Heremans, and S. Rajan, Applied Physics Letters 112 (17) (2018), with the permission of AIP Publishing. 17

The electron scattering was found to be dominated by impurity scattering at low temperature, and by polar optical phonon scattering in the high temperature range. A significant improvement of the low-temperature mobility was observed when the UID β-Ga₂O₃ buffer layer thickness was increased from 130 nm to 360 nm. Mobility calculation suggested a corresponding reduction of the background impurity concentration through the growth of thicker buffer layer. At low temperatures, mobility is limited by a combination of interface roughness and background impurity scattering. Further optimization of the epitaxial material quality is expected to further increase the 2DEG mobility at low temperatures. Recently, the development of growth techniques, such as MOCVD³⁹ and HVPE⁴¹, has led to high quality epitaxial layers with low background charge concentrations below 10¹⁶ cm ³, and therefore, low-temperature electron mobility above 5000 cm²/Vs was demonstrated.⁴¹ However, the difference in the background impurity concentration showed minimal impact on the room-temperature mobility, which is intrinsically limited by the low optical phonon energy. 42,43 Increasing the 2DEG density to take advantage of the enhanced screening effect provides a viable solution to overcome such mobility limits²¹.

The high channel mobility at low temperature and the existence of a degenerate 2DEG allowed for the observation of quantum transport in the Ga_2O_3 material system. The dependence of the transverse magnetoresistance (R_{xx}) of the modulation doped structure on the magnetic field perpendicular to the sample surface was measured, as shown in Fig. 3. Multiple periods of oscillations were observed for the transverse magnetoresistance (R_{xx}), and plateaus corresponding to Landau splitting were observed in the measured Hall resistance (R_{xy}). These results represent the first demonstration of Shubnikov-de Haas oscillations in the Ga2O3 material system.¹⁷

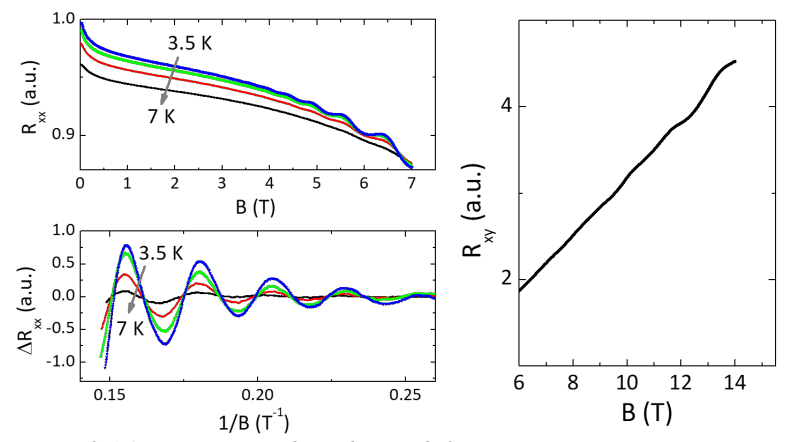


Figure 3 (a) Temperature dependence of the transverse magnetoresistance of a Al-GaO/GaO 2DEG channel as a function of the magnetic field perpendicular to the sample surface. (b) SdH oscillations of the transverse magnetoresistances. (c) The Hall resistances (Rxy) of the channel showing plateaus, which corresponds to the quantization of Landau levels. Reproduced from Y. Zhang, A. Neal, Z. Xia, C. Joishi, J. Johnson, Y. Zheng, S. Bajaj, M. Brenner, D. Dorsey, K. Chabak, G. Jessen, J. Hwang, S. Mou, J. Heremans, and S. Rajan, Applied Physics Letters 112 (17) (2018), with the permission of AIP Publishing. 17

The oscillation component of R_{xx} was extracted by subtracting the non-oscillating background, and was plotted as a function of reciprocal magnetic field (1/B) as shown in Fig. 3. The oscillation period $\Delta(1/B)$ is determined by the 2DEG carrier density through the expression: $\Delta(1/B) = e/\pi\hbar n_{2D}$. The carrier density extracted from the SdH oscillations is 1.96×10^{12} cm⁻², which matches well with the low-field Hall measurements.

The first observation of quantum oscillations suggests that the β -(Al_xGa₁, x)₂O₃/Ga₂O₃ modulation-doped structure could be a great platform for the studies of quantum transport in the material system. This could be used for the extraction of a range of fundamental material properties and investigate novel quantum phenomena in β-Ga₂O₃. The electron effective mass could be extracted based on the SdH oscillation amplitude as a function of the measurement temperature. The fitting to the experimental data suggested an effective mass of m^* = 0.313 ± 0.015 m_0 , which is close to what was estimated from the theoretical calculations, band structure measurements and optical Hall measurements. At the same time, the quantum scattering time could be extracted to be 0.33 ps. This provides a reference for the analysis of the dominating scattering mechanism for low field electron transport in β-Ga₂O₃.¹⁷

As discussed above, further increasing the 2DEG density in a single AlGaO/GaO heterostructure is challenging because of the limited conduction band offset that can be obtained in the present growth technologies. Two major solutions are possible to

increase the 2DEG density. The first one is to develop novel growth conditions to increase Al incorporation. Higher growth temperature was found to be favorable for the stability of AlGaO in the monoclinic phase. There are now significant research efforts toward higher temperature growth of AlGaO using both MOCVD and MBE.^{28,34} A recent demonstration of an In-catalyzed AlGaO growth method pushed the MBE growth temperature to more than 200 °C higher than the typical growth temperatures, which provides a tremendous growth window to explore.²⁸ However, heterostructures with higher Al compositions have not been demonstrated. A second method to increase the 2DEG density is to introduce multiple heterostructures.¹⁵

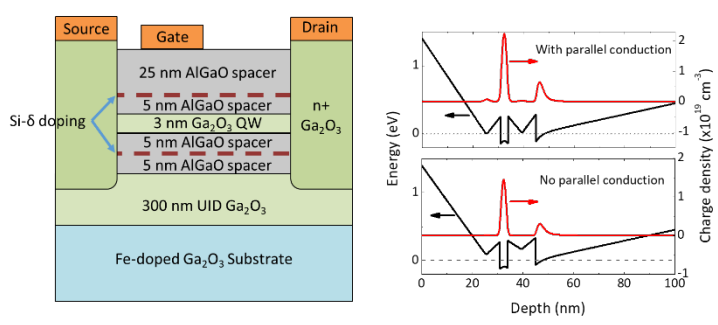


Figure 4 (a) Schematic epitaxial stack of the double heterostructure MODFET. (b) Equilibrium energy band diagrams with and without parasitic channel and the corresponding 2DEG charge distributions. Reproduced from Y. Zhang, C. Joishi, Z. Xia, M. Brenner, S. Lodha, and S. Rajan, Applied Physics Letters 112 (23), 233503 (2018), with the permission of AIP Publishing. ¹⁵

Y. Zhang et al demonstrated experimentally 15 a double heterostructure as shown in Fig. 4. Compared to the single heterostructure, the electrons are confined in a GaO quantum well layer sandwiched between two AlGaO barrier layers. Since Si delta doping exists in both AlGaO layers, electrons could be transferred from both below and above the β -Ga₂O₃ quantum well, resulting in a higher achievable 2DEG density in the quantum well. Using this structure, a confined 2DEG charge density of 3.85×10^{12} cm⁻² was estimated from low-temperature Hall measurement, which doubled what was achievable in a single heterostructure. The experimental confirmation of higher 2DEG density in the double heterostructure suggests that further charge scaling is feasible by increasing the number of quantum wells. This provides an elegant method to reach high charge densities required for high current and high power device operations.

The field effect mobility of the quantum well channel was evaluated using three-terminal measurement on a fat transistor with gate length/ width of $L_G/W=100/100$ µm. The field effect mobility was found to peak at 150 cm²/Vs in the β -Ga₂O₃ quantum well layer as shown in Fig. 5, however, it showed a significant reduction to 35 cm²/Vs in the β -(Al_xGa_{1-x})₂O₃ layers, which could be limited by the strong ionized impurity scattering and alloy scattering in the parasitic channel in the AlGaO layer.

The field effect mobility could be translated to Hall mobility by multiplying with the Hall factor, which was estimated to be ~ 1.7 by N. Ma et al.⁴² This leads to a Hall mobility of 255 cm²/Vs, which is higher than the measured Hall mobility of 180 cm²/Vs in a single heterostructure, and further confirms the enhanced screening effect on the scattering centers, especially the polar optical phonons, by increasing the 2DEG density.¹⁵

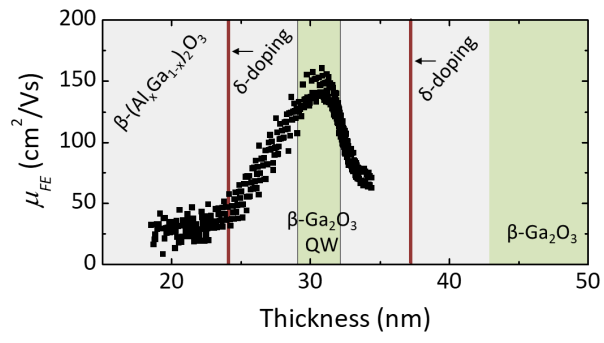


Figure 5 Depth profile of the field effect mobility (μ_{FE}) extracted from a fat transistor at V_{DS} =0.1 V. Reproduced from Y. Zhang, C. Joishi, Z. Xia, M. Brenner, S. Lodha, and S. Rajan, Applied Physics Letters 112 (23), 233503 (2018), with the permission of AIP Publishing. ¹⁵

Modulation-doped Field Effect transistors

AlGaO/GaO modulation-doped structure holds great promise for both high frequency and high-power device applications, mainly because of the excellent transport properties and the feasiblity for aggressive device scaling in both the vertical and the lateral directions. Preliminary device demonstrations on modulation doped field effect transistors were reported by Krishnamoorthy et al¹⁶ and Ahmadi et al¹³, however, the device performance was compromised by the poor contacts and the dominant parasitic channel in the AlGaO barrier layer. Recently, AlGaO/GaO single heterostructure MODFETs with pure 2DEG channel was demonstrated by Zhang et al.^{15,17,36} Using Pt/Au Schottky gate contact, the device showed normally-off operation because of the depletion of the low 2DEG charge density ~ 2×10¹² cm⁻² under the gate.

As shown in Fig. 6, the MODFET device showed excellent drain current on/off ratio above 10^9 . The subthreshold slope is ~ 90 mV/decade over more than five decades of the subthreshold current, suggesting high material quality of the β -(Al_xGa_{1-x})₂O₃ barrier layer. The devices showed low output conductance after saturation, indicating good gate control of the 2DEG channel. The peak transconductance (g_m) was measured to be 39 mS/mm at (V_{DS} , V_{GS}) of (10 V, 1.5 V) for the device with a gate length (L_G) of 0.7 μ m. While the transconductance is still limited by the low channel mobility because of the long channel length and low charge density,

the obtained transconductance is among the highest reported values for Ga_2O_3 transistors. The drain current of the devices was limited by the low charge density of 2×10^{12} cm⁻², and higher drain current above 250 mA/mm was achieved for double heterostructure MODFETs by increasing the total channel charge density. ¹⁵

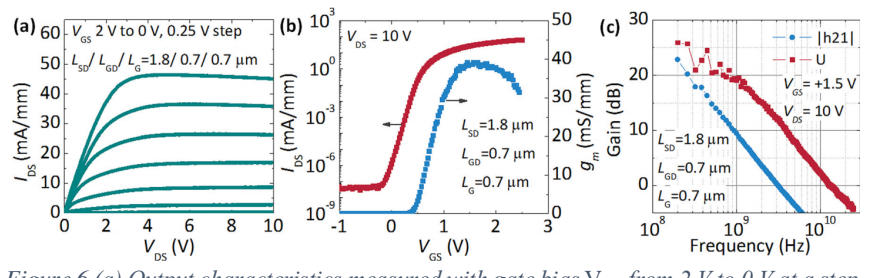


Figure 6 (a) Output characteristics measured with gate bias V_{GS} from 2 V to 0 V at a step of 0.25 V. (b) Transfer characteristics measured under a drain bias of V_{DS} =10 V. (c) RF characteristics measured at V_{DS} =10 V and V_{GS} =1.5 V. The gate length, gate-drain spacing, source-drain spacing of the device are L_G =0.7 μ m, L_{GD} =0.7 μ m and L_{SD} =1.8 μ m, respectively. Reproduced from Y. Zhang, A. Neal, Z. Xia, C. Joishi, J. Johnson, Y. Zheng, S. Bajaj, M. Brenner, D. Dorsey, K. Chabak, G. Jessen, J. Hwang, S. Mou, J. Heremans, and S. Rajan, Applied Physics Letters 112 (17) (2018), with the permission of AIP Publishing. 17

The RF performance of the β-(Al_xGa_{1-x})₂O₃/Ga₂O₃ MODFETs was characterized as shown in Fig. 6(c). The small-signal measurements on the MODFET device with L_G =0.7 μ m showed a cutoff frequency of 3.1 GHz, and maximum oscillation frequency of 13.1 GHz at V_{DS} of 10 V and V_{GS} of 1.5 V. Compared to AlGaN/GaN HEMTs or AlGaAs/GaAs MODFETs with similar gate length, the high frequency performance of β-(Al_xGa_{1-x})₂O₃/Ga₂O₃ MODFETs is still limited due to the lower channel mobility, which prevents electrons from reaching saturated velocity. However, due to the significant increase in the 2DEG mobility at low temperatures (as shown in Fig. 2), it is in fact possible to achieve velocity saturation inside the channel at lower temperatures. The small signal RF measurement of a β-(Al_xGa₁- $_{\rm x}$)₂O₃/Ga₂O₃ MODFET device with gate length of $L_G = 0.61 \, \mu \rm m$ indicated a significant increase in the both f_t and f_{max} from 4.0/ 11.8 GHz at room temperature to 17.4/ 40.8 GHz at 50 K. The analysis of the low temperature f_t based on device simulations indicated a peak velocity of 1.2×10⁷ cm/s.³⁶ The current gain cut-off frequency is comparable to the GaN devices with similar gate length, further suggesting that the saturation velocity in β-Ga₂O₃ is comparable to that in GaN.

Three terminal off-state breakdown measurements of AlGaO/GaO MODFETs suggested a breakdown voltage of 122.4 V for the device with gate-drain spacing of $L_{GD} = 0.38~\mu m$. This translates into an average breakdown field of 3.22 MV/cm. Further incorporation of SiO₂ dielectric layer for field management has led to improved breakdown field near 4 MV/cm and high breakdown voltages above 1 kV for the AlGaO/GaO MODFETs.⁴⁴

Summary

The design and development of 2DEG channels in AlGaO/GaO modulation-doped structures was reviewed in this chapter. While the research on modulation doping in the β -Ga₂O₃ system is still in its early stage, tremendous progress has been achieved. The main results are summarized below.

- 1. Improved transport properties were observed for 2DEG channels as compared to the bulk doped channels. The room temperature mobility was found to be $180\,\text{cm}^2/\text{Vs}$ in AlGaO/GaO single heterostructures, while the estimated Hall mobility reached 255 cm²/Vs in the quantum well channel of the double heterostructure MODFETs. The low temperature mobility of 2790 cm²/Vs (50 K) measured in the 2DEG channel is within the highest reported mobility values in $\beta\text{-Ga}_2\text{O}_3$ regardless of a high background charge estimated to be $\sim 10^{17}~\text{cm}^{-3}$ in the channel region. Further improvement of the material quality and reduction of the impurity concentration could lead to substantial improvement in the low-temperature mobility, making it possible to investigate quantum transport characteristics in $\beta\text{-Ga}_2\text{O}_3$.
- 2. Due to the high channel mobility 2DEG, quantum oscillations were observed in β -Ga₂O₃ for the first time. The analysis of the oscillation amplitude as a function of the measurement temperature and magnetic field led to the extraction of the effective mass to be m^* = 0.313 ± 0.015 m_0 and quantum scattering time to be 0.33 ps.
- 3. The high channel mobility at low temperatures made it possible to extract the electron saturation velocity in β -Ga₂O₃. A saturation velocity of 1.2×10^7 cm/s was estimated based on both the measured velocity-field profile and the analysis on the small-signal RF measurements at 50 K, which showed a current gain cutoff frequency of 17.4 GHz for the device with gate length of 0.61 μ m.
- 4. The 3-terminal off states breakdown measurements on the MODFETs suggested high average breakdown fields near 4 MV/cm.

The experimental confirmation of the enhanced transport properties, high saturation velocity and high breakdown field in the AlGaO/GaO MODFETs makes them promising candidates for future electronic device applications.

References:

- M. Orita, H. Ohta, M. Hirano, and H. Hosono, Applied Physics Letters 77 (25), 4166 (2000).
- M. Higashiwaki, K. Sasaki, A. Kuramata, T. Masui, and S. Yamakoshi, Applied Physics Letters **100** (1), 013504 (2012).
- K. Ghosh and U. Singisetti, Journal of Applied Physics 122 (3), 035702 (2017).

- H. Aida, K. Nishiguchi, H. Takeda, N. Aota, K. Sunakawa, and Y. Yaguchi, Japanese Journal of Applied Physics **47** (11R), 8506 (2008).
- Y. Tomm, J. Ko, A. Yoshikawa, and T. Fukuda, Journal of crystal growth **66** (1-4), 369 (2001).
- Y. Tomm, P. Reiche, D. Klimm, and T. Fukuda, Journal of crystal growth **220** (4), 510 (2000).
- M. Higashiwaki, K. Sasaki, T. Kamimura, M. Hoi Wong, D. Krishnamurthy, A. Kuramata, T. Masui, and S. Yamakoshi, Applied Physics Letters **103** (12), 123511 (2013).
- A. J. Green, K. D. Chabak, M. Baldini, N. Moser, R. Gilbert, R. C. Fitch, G. Wagner, Z. Galazka, J. Mccandless, and A. Crespo, IEEE Electron Device Letters **38** (6), 790 (2017).
- M. H. Wong, K. Sasaki, A. Kuramata, S. Yamakoshi, and M. Higashiwaki, IEEE Electron Device Letters 37 (2), 212 (2016).
- N. Moser, J. McCandless, A. Crespo, K. Leedy, A. Green, A. Neal, S. Mou, E. Ahmadi, J. Speck, and K. Chabak, IEEE Electron Device Letters **38** (6), 775 (2017).
- S. Krishnamoorthy, Z. Xia, S. Bajaj, M. Brenner, and S. Rajan, Applied Physics Express **10** (5), 051102 (2017).
- W. S. Hwang, A. Verma, H. Peelaers, V. Protasenko, S. Rouvimov, H. Xing, A. Seabaugh, W. Haensch, C. V. de Walle, and Z. Galazka, Applied Physics Letters **104** (20), 203111 (2014).
- E. Ahmadi, O. S. Koksaldi, X. Zheng, T. Mates, Y. Oshima, U. K. Mishra, and J. S. Speck, Applied Physics Express **10** (7), 071101 (2017).
- Y. Zhang, A. Neal, Z. Xia, C. Joishi, J. Johnson, Y. Zheng, S. Bajaj, M. Brenner, D. Dorsey, K. Chabak, G. Jessen, J. Hwang, S. Mou, J. Heremans, and S. Rajan, Applied Physics Letters **112** (17) (2018).
- Y. Zhang, C. Joishi, Z. Xia, M. Brenner, S. Lodha, and S. Rajan, Applied Physics Letters **112** (23), 233503 (2018).
- S. Krishnamoorthy, Z. Xia, C. Joishi, Y. Zhang, J. McGlone, J. Johnson, M. Brenner, A. R. Arehart, J. Hwang, and S. Lodha, Applied Physics Letters **111** (2), 023502 (2017).
- Y. Zhang, A. Neal, Z. Xia, C. Joishi, J. M. Johnson, Y. Zheng, S. Bajaj, M. Brenner, D. Dorsey, and K. Chabak, Applied Physics Letters 112 (17), 173502 (2018).
- C. Joishi, S. Rafique, Z. Xia, L. Han, S. Krishnamoorthy, Y. Zhang, S. Lodha, H. Zhao, and S. Rajan, Applied Physics Express 11 (3), 031101 (2018).
- K. Konishi, K. Goto, H. Murakami, Y. Kumagai, A. Kuramata, S. Yamakoshi, and M. Higashiwaki, Applied Physics Letters 110 (10), 103506 (2017).
- A. J. Green, K. D. Chabak, E. R. Heller, R. C. Fitch, M. Baldini, A. Fiedler, K. Irmscher, G. Wagner, Z. Galazka, and S. E. Tetlak, IEEE Electron Device Letters **37** (7), 902 (2016).

- K. Ghosh and U. Singisetti, Journal of Materials Research **32** (22), 4142 (2017).
- H. Peelaers, J. B. Varley, J. S. Speck, and C. G. Van de Walle, Applied Physics Letters **112** (24), 242101 (2018).
- T. Mimura, S. Hiyamizu, T. Fujii, and K. Nanbu, Japanese journal of applied physics **19** (5), L225 (1980).
- B. W. Krueger, C. S. Dandeneau, E. M. Nelson, S. T. Dunham, F. S. Ohuchi, and M. A. Olmstead, Journal of the American Ceramic Society **99** (7), 2467 (2016).
- S. W. Kaun, F. Wu, and J. S. Speck, Journal of Vacuum Science & Technology A: Vacuum, Surfaces, and Films **33** (4), 041508 (2015).
- T. Oshima, T. Okuno, N. Arai, Y. Kobayashi, and S. Fujita, Japanese Journal of Applied Physics **48** (7R), 070202 (2009).
- Q. Feng, X. Li, G. Han, L. Huang, F. Li, W. Tang, J. Zhang, and Y. Hao, Optical Materials Express 7 (4), 1240 (2017).
- P. Vogt, A. Mauze, F. Wu, B. Bonef, and J. S. Speck, Applied Physics Express 11 (11), 115503 (2018).
- F. Zhang, K. Saito, T. Tanaka, M. Nishio, M. Arita, and Q. Guo, Applied Physics Letters **105** (16), 162107 (2014).
- ³⁰ X. Wang, Z. Chen, F. Zhang, K. Saito, T. Tanaka, M. Nishio, and Q. Guo, AIP Advances **6** (1), 015111 (2016).
- C. Kranert, M. Jenderka, J. Lenzner, M. Lorenz, H. von Wenckstern, R. Schmidt-Grund, and M. Grundmann, Journal of Applied Physics **117** (12), 125703 (2015).
- R. Schmidt-Grund, C. Kranert, H. Von Wenckstern, V. Zviagin, M. Lorenz, and M. Grundmann, Journal of Applied Physics **117** (16), 165307 (2015).
- H. Ito, K. Kaneko, and S. Fujita, Japanese Journal of Applied Physics **51** (10R), 100207 (2012).
- R. Miller, F. Alema, and A. Osinsky, IEEE Transactions on Semiconductor Manufacturing **31** (4), 467 (2018).
- T. Oshima, Y. Kato, N. Kawano, A. Kuramata, S. Yamakoshi, S. Fujita, T. Oishi, and M. Kasu, Applied Physics Express **10** (3), 035701 (2017).
- Y. Zhang, Z. Xia, J. McGlone, W. Sun, C. Joishi, A. R. Arehart, S. A. Ringel, and S. Rajan, IEEE Transactions on Electron Devices **66**, 1574 (2019).
- ³⁷ Z. Xia, C. Joishi, S. Krishnamoorthy, S. Bajaj, Y. Zhang, M. Brenner, S. Lodha, and S. Rajan, IEEE Electron Device Letters **39** (4), 568 (2018).
- T. Oishi, Y. Koga, K. Harada, and M. Kasu, Applied Physics Express **8** (3), 031101 (2015).
- Y. Zhang, F. Alema, A. Mauze, O. S. Koksaldi, R. Miller, A. Osinsky, and J. S. Speck, APL Materials 7 (2), 022506 (2019).
- S. Rafique, M. R. Karim, J. M. Johnson, J. Hwang, and H. Zhao, Applied Physics Letters **112** (5), 052104 (2018).

- K. Goto, K. Konishi, H. Murakami, Y. Kumagai, B. Monemar, M. Higashiwaki, A. Kuramata, and S. Yamakoshi, Thin Solid Films **666**, 182 (2018).
- N. Ma, N. Tanen, A. Verma, Z. Guo, T. Luo, H. Xing, and D. Jena, Applied Physics Letters **109** (21), 212101 (2016).
- Y. Kang, K. Krishnaswamy, H. Peelaers, and C. G. Van de Walle, Journal of Physics: Condensed Matter **29** (23), 234001 (2017).
- 44 C. Joishi, Y. Zhang, Z. Xia, W. Sun, A. R. Arehart, S. A. Ringel, S. Lodha, and S. Rajan, Submitted to IEEE Electron Device Letters (2019).